Synthesis and characterization of superconducting single-crystal Sn nanowires

Mingliang Tian,[a),b)] Jinguo Wang, Joseph Snyder,[a)] James Kurtz,[a)] Ying Liu,[a)] Peter Schiffer,[a)] Thomas E. Mallouk,[c)] and M. H. W. Chan[a)]
The Materials Research Institute and The Center for Nanoscale Science (MRSEC), Pennsylvania State University, University Park, Pennsylvania 16802-6300

(Received 29 April 2003; accepted 16 June 2003)

Single-crystal superconducting tin nanowires with diameters of 40–160 nm have been prepared by electrochemical deposition in porous polycarbonate membranes. Structural characterization through transmission electron microscopy and x-ray diffraction showed that the nanowires are highly oriented along the [100] direction. Although the superconducting transition temperature is close to the bulk value of 3.7 K, the effect of reduced dimensionality is clearly evident in the electrical transport properties of the thinnest wires (40 nm diameter). Magnetization measurements show that the critical field of the nanowires increases significantly with decreasing diameter to ~0.3 T for the thinnest wires, nearly an order of magnitude larger than the bulk value. © *2003 American Institute of Physics.* [DOI: 10.1063/1.1601692]

When the physical dimension of a superconductor becomes comparable to or smaller than the temperature-dependent coherence length $\xi(T)$, its properties of a superconductor are expected to change significantly,[1–12] including suppression of the superconducting transition temperature (T_C)[5,6] and finite residual resistance at low temperatures.[8–12] The suppression of T_C in homogenous nanowires was attributed to the enhanced Coulomb interaction in one dimension (1D),[13] and the finite resistance seen at low temperatures may be related to the presence of weak links between the grains[14] or the quantum phase-slip process.[8,9,15]

Since the most detailed work in 1D or two-dimensional superconducting systems has been carried out in polycrystalline or amorphous samples,[1–12] our understanding of the nature of superconductivity is often limited by the sample's morphology (e.g., disorder, defects, grain boundaries, or crystallinity). In order to identify the intrinsic phenomena in 1D, experimental studies of single crystal nanowires are clearly desirable. Yi *et al.*[16] fabricated Pb single-crystal nanowires by pulse electrodeposition. They found that the transition temperature in single crystal wires is close to the bulk T_C, but significantly suppressed in polycrystalline wires. Resistance and magnetization as a function of magnetic field or temperature for Pb wires were also measured by Dubois *et al.*[17] and Michotte *et al.*[18] They found superconductivity of Pb nanowires survives only in thicker polycrystalline wires (i.e., for diameters >50 nm) with single-crystal segments. The length of the single-crystal segments varies within a few microns, while the total length of the wires is on the order of 25 μm. In these wires, the critical field is found to increase monotonically with decreasing diameter. For wires of diameter below 50 nm, resistance is found to increase with decreasing temperature below 10 K, with no evidence of superconductivity. The insulating behavior in thin Pb wires was attributed by the authors to be related to the ''poor crystal structure;'' that is, a lacking of electron diffraction pattern. These experiments further confirm the need of measurement on single-crystal wires of the smallest diameters.

We report the fabrication, characterization, and physical properties of single-crystal tin wires of diameters $d \sim 40-160$ nm made by electrodeposition in porous membranes, the same method used by Dubois *et al.*[17] and Michotte *et al.*[18] We chose tin in our studies because bulk tin has a relatively long coherence length of $\xi(0) \sim 200$ nm. We found that all single-crystal Sn nanowires studied showed superconducting transition near 3.7 K, which is close to the critical temperature of bulk tin (3.73 K), but both the electrical transport properties below T_C and the critical field exhibit effects of reduced dimensionality.

Our nanowires were grown in commercially available ''track etched'' polycarbonate membranes. The pores in these membranes are 1D channels with quoted pore diameters of 10, 30, 50, and 80 nm, respectively, and are aligned perpendicular to the face of the membrane within $\pm 17°$. The thickness and pore density of the membranes are 6 μm and 6 $\times 10^8$ pores/cm^2, respectively. The electrolyte used for electrodeposition was 0.l M Sn_2SO_4 aqueous solution with 2% gelatin by weight, and the *p*H value was adjusted to be near 1 with concentrated H_2SO_4. Before electrodeposition, a 200-nm Au film was evaporated onto one side of the membrane that served as the conducting cathode. A pure tin wire was used as the anode, and electroplating was done under a constant voltage of -80 mV using a two-electrode system in a quartz tube cell at room temperature. The nanowires could be collected by dissolving the polycarbonate membrane in dichloromethane and precipitating them from the solvent by the use of a centrifuge. The freestanding nanowires could then be stored in suspension in *n*-ethyl alcohol.

Structural characterization of the resulting nanowires was carried out by high-resolution transmission electron microscopy (HRTEM) and by electron diffraction (ED) in a

[a)]Also at Department of Physics, Penn State University.
[b)]Electronic mail: tian@phys.psu.edu
[c)]Also at Department of Chemistry, Penn State University.

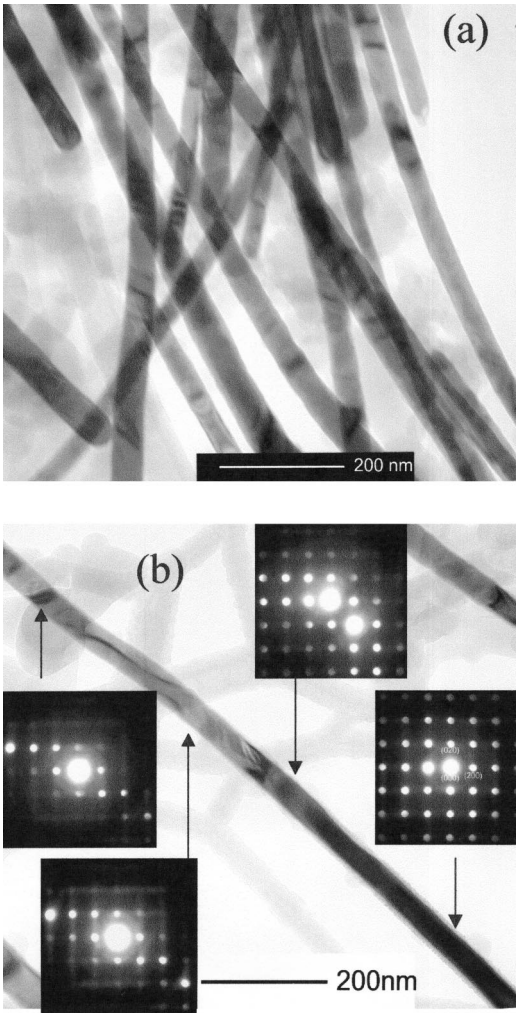

FIG. 1. (a) TEM image of freestanding 40-nm Sn nanowires. (b) TEM image of a selected 40-nm Sn nanowire and its ED patterns along the wire length.

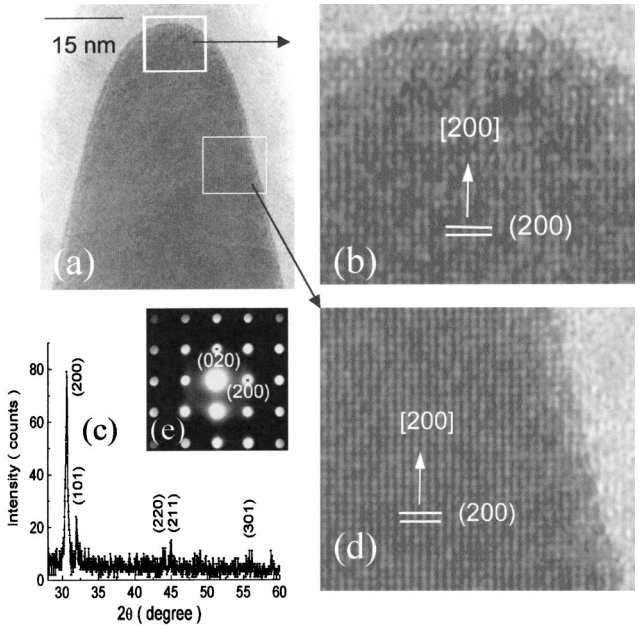

FIG. 2. (a) HRTEM image of the growth tip of a Sn nanowire; (b) and (d) are the magnified images of local regions of the tip marked by the two boxes; (c) and (e) are, respectively, the XRD spectra of large scale Sn nanowires array and the ED pattern of the tip.

FH-2000 field-emission TEM. Figure 1(a) shows the TEM image of freestanding Sn nanowires harvested from polycarbonate membrane with quoted pore size of 10 nm. The actual diameter is 40 ± 5 nm, four times larger than the nominal pore diameter reported by the manufacturer. Similarly, the average diameters of the nanowires deposited into membranes with nominal pore diameters of 30, 50, and 80 nm are about 70, 100, and 168 nm, respectively. The diameters of individual wires were found to be very uniform for the 40- and 70-nm wires. The diameter could vary as much as 15% along the length of wires with diameters of 100 and 168 nm, which is consistent with the finding of Schonenberger *et al.*[19]

Figure 1(b) shows the TEM image of a randomly selected 40-nm Sn nanowire and ED patterns of the same wire along its length. The diffraction pattern does not change along the length of the wire except for a gradual variation in the intensity of the diffraction spots, suggesting that the nanowire is single crystal. The variation in the intensity of ED pattern along the length might be related to a slight deformation of the wire, which may be created during the process of release from the membrane. Analysis of the ED pattern showed that the growth direction of this wire was along the [100] crystallographic direction of tetragonal β-tin. The locally enlarged HRTEM images and the ED pattern shown in Fig. 2 also clearly demonstrate single-crystal structure with [100] orientation. About 90% of the wires had the preferred [100] growth direction, while most of the others grew in the [110] direction. An oxidized layer with a thickness of 5–8 nm was observed on the surface of the wire and was somewhat thicker near the tip.

An x-ray diffraction (XRD) pattern of a piece of polycarbonate membrane containing an array of Sn nanowires is shown in Fig. 2(c). The intensity of the (200) peak for the as-made nanowires is almost 3.5 times higher than that of the secondary (101) peak. The ratio of the intensities of the (200) and (101) peaks for polycrystalline β-tin powder is expected to be 1.1. This result confirms our TEM data that the growth direction of Sn nanowires in the channels is highly preferred along the [100] direction.

Resistance measurements were performed on an array of Sn nanowires. The arrangement of the system is shown schematically in the inset of Fig. 3(a). High-purity bulk tin wires (99.999%) of 0.5 mm in diameter were mechanically squeezed onto the two sides of the membrane, which were used as the current and voltage leads. With this arrangement, the series contact resistance can be neglected below the transition temperature of bulk tin, and other features in the data below the bulk T_C can be attributed to the nanowires.

Figure 3(a) shows the $R(T)$ curves of 40-, 70-, and 100-nm tin nanowires measured with a small dc current. The resistance data for all three sizes of single-crystal wires show an onset of superconducting transition near 3.7 K, the bulk T_C of tin. The resistance drop for the 70 and 100 nm wires is sharp; their resistance falls from the normal value to zero within our measurement accuracy (3 nV/1 μA), in a temperature interval of 90 mK. Quite different behavior is observed for the 40-nm wires; namely, a gradual drop in resistance with decreasing temperature. The data for this sample exhibit two distinct regimes below T_C, one between 1.7 and 3 K,

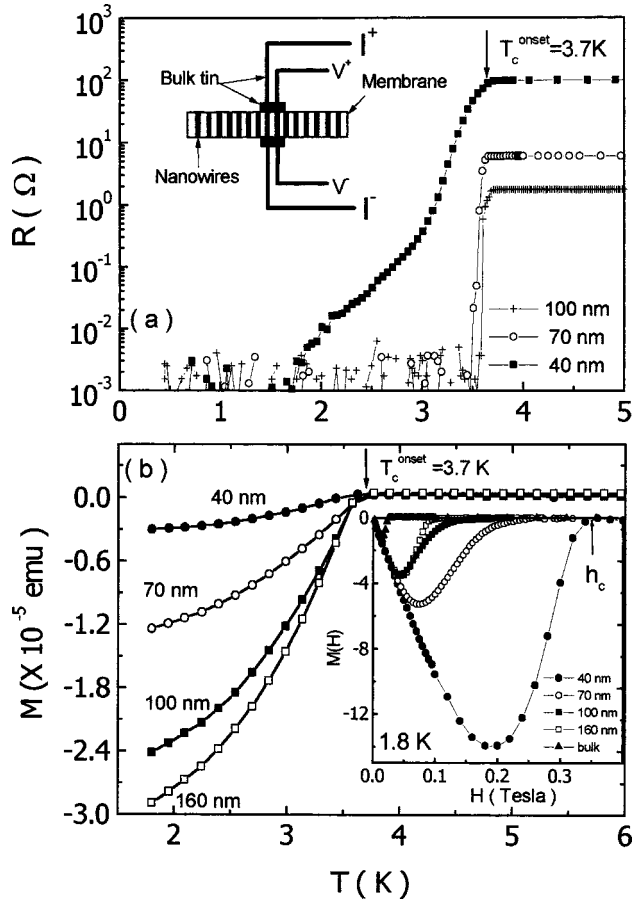

FIG. 3. (a) $R-T$ curves of 40-, 70-, and 100-nm Sn nanowire array; the inset shows the schematic of the measurement arrangement. (b) $M-T$ curves of 40-, 70-, 100-, and 160-nm Sn nanowire array measured at 0.01-T magnetic field along the wire axis. The inset shows the $M(H)$ curves of the Sn nanowire array with various diameters at 1.8 K.

and another between 3 and 3.7 K. The overall resistive behavior of the 40-nm Sn wire is similar to that found by Giordano in thin In-Pb wires. The temperature dependence of the resistance of the In-Pb wires below T_C was interpreted by Giordano as a superposition of thermally activated phase-slip resistance near T_C,[20] plus quantum phase-slip (QPS) far below T_C.[8,9] The interpretation of Giordano may also be applicable to our result in 40-nm Sn wires. A systematic transport study on thinner wires is currently in progress.

Magnetization (M) of the nanowire arrays was also measured. The magnetic field was applied perpendicular to the membrane and hence parallel to the wire axes within $\pm 17°$. Figure 3(b) shows $M(T)$ for 40, 70, 100, and 160-nm Sn wires measured with a field of 0.01 T. Since the total mass of the nanowire array inside the membrane cannot be determined precisely, the data are not normalized by the mass of the nanowires. The data show clear diamagnetic behavior below the bulk transition temperature of 3.7 K, which is in good agreement with the data of the electrical transport measurement.

The inset of Fig. 3(b) shows $M(H)$ data for different diameter nanowire arrays at 1.8 K, where the data in each curve were normalized by the value at $H=0.01$ T. The $M(H)$ curve of bulk tin is also shown in the inset for comparison. It is seen that each $M-H$ curve for Sn nanowires shows a diamagnetic valley peak, and the transition range from the superconducting to normal state is very broad. The onset critical field h_c, indicated by the arrow in the inset of Fig. 3(b), was found to increase significantly with decreasing diameter. The h_c for 40 nm is found to be ~ 0.3 T at 1.8 K, an order of magnitude higher than that of bulk Sn. These results are consistent with the observation of Dubois *et al.*[17] and Michotte *et al.*[18] in Pb wires. However, the $M(T)$ and $M(H)$ curves in our single-crystal tin wires did not show the irreversibility or hysteretic behavior observed in the Pb wires. The reversible $M(H)$ curves of tin wires indicates a lack of pinning of residual flux in contract to the interpretation of Ref. 18 in Pb wires.

In summary, the broadening of the superconducting transition and the resistive tail well below T_C observed in 40-nm single crystal wires suggest that we are approaching the limit of 1D behavior. Our results indicate single-crystal tin nanowires of smaller diameter show promise in elucidating the nature of 1D superconductivity.

The authors acknowledge useful discussions with Jong E. Han, Mari-Anne M. Rosario, Vincent Crespi, and Jainendra Jain. This work is supported by Penn State MRSEC Fund Nos. DMR-0080019 and DMR-0213623.

[1] A. K. Geim, S. V. Dubonos, J. G. S. Lok, M. Henini, and J. C. Maan, Nature (London) **396**, 144 (1998).
[2] Y. Liu, Yu. Zadorozhny, M. M. Rosario, B. Y. Rock, P. T. Carrigan, and H. Wang, Science **294**, 2332 (2001).
[3] D. C. Ralph, C. T. Black, and M. Tinkham, Phys. Rev. Lett. **78**, 4087 (1997).
[4] P. Santhanam, C. P. Umbach, and C. C. Chi, Phys. Rev. B **40**, 11392 (1989).
[5] J. M. Graybeal, P. M. Mankiewich, R. C. Dynes, and M. R. Beasley, Phys. Rev. Lett. **59**, 2697 (1987).
[6] F. Sharifi, A. V. Herzog, and R. C. Dynes, Phys. Rev. Lett. **71**, 428 (1993).
[7] A. Bezryadin, C. N. Lau, and M. Tinkham, Nature (London) **404**, 971 (2000).
[8] C. N. Lau, N. Markovic, M. Bockrath, A. Bezryadin, and Tinkham, Phys. Rev. Lett. **87**, 217003 (2001).
[9] N. Giordano, Phys. Rev. Lett. **61**, 2137 (1988); Phys. Rev. B **41**, 6350 (1990); **43**, 160 (1991).
[10] R. P. Barber, Jr. and R. C. Dynes, Phys. Rev. B **48**, 10618 (1993); **49**, 3409 (1994).
[11] A. V. Herzog, P. Xiong, F. Sharifi, and R. C. Dynes, Phys. Rev. Lett. **76**, 668 (1996).
[12] A. V. Herzog, P. Xiong, and R. C. Dynes, Phys. Rev. B **58**, 14199 (1998).
[13] Y. Oreg and A. M. Finkel'stein, Phys. Rev. Lett. **83**, 191 (1999).
[14] J. M. Duan, Phys. Rev. Lett. **74**, 5128 (1995).
[15] A. D. Zaikin, D. S. Golubev, A. van Otterlo, and G. T. Zimanyi, Phys. Rev. Lett. **78**, 1552 (1997).
[16] G. Yi and W. Schwarzacher, Appl. Phys. Lett. **74**, 1746 (1999).
[17] S. Dubois, A. Michel, J. P. Eymery, J. L. Duvail, and L. Piraux, J. Mater. Res. **14**, 665 (1999).
[18] S. Michotte, L. Piraux, S. Dubois, F. Pailloux, G. Stenuit, and J. Govaerts, Physica C **377**, 267 (2002).
[19] C. Schonenberger, B. M. I. van der Zande, L. G. J. Fokkink, M. Henny, C. Schmid, M. Kruger, A. Bachtol, R. Huber, H. Birk, and U. Staufer, J. Phys. Chem. B **101**, 5497 (1997).
[20] J. S. Langer and V. Ambegaokar, Phys. Rev. **164**, 498 (1967); D. E. McCumber and B. I. Halperin, Phys. Rev. B **1**, 1054 (1970).